

Geophysical Research Letters



RESEARCH LETTER

10.1029/2021GL094137

Key Points:

- Simulations including time-varying large-scale forcing and open boundaries may improve representation of shallow cumulus fields
- Aerosol effects on shallow cumuli may be constrained by large-scale forcing, but nonetheless significant
- Met Office Unified Model (UM) allows for a variety of configurations to compare modelling approaches

Correspondence to:

G. Spill,
george.spill@physics.ox.ac.uk

Citation:



Spill, G., Stier, P., Field, P. R., & Dagan, G. (2021). Contrasting responses of idealised and realistic simulations of shallow cumuli to aerosol perturbations. *Geophysical Research Letters*, 48, e2021GL094137. <https://doi.org/10.1029/2021GL094137>

Received 9 FEB 2021

Accepted 16 JUN 2021

Revised 26 MAY 2021

Contrasting Responses of Idealised and Realistic Simulations of Shallow Cumuli to Aerosol Perturbations

George Spill¹ , Philip Stier¹ , Paul R. Field^{2,3} , and Guy Dagan¹ 

¹Atmospheric, Oceanic and Planetary Physics, Department of Physics, University of Oxford, Oxford, UK, ²Met Office, Exeter, UK, ³Institute of Climate and Atmospheric Science, School of Earth and Environment, University of Leeds, Leeds, UK

Abstract Shallow clouds remain greatly significant in improving our understanding of the atmosphere. Using the Met Office Unified Model, we compare highly idealised simulations of shallow cumuli with those using more realistic domains, with open lateral boundaries and varying large-scale forcing. We find that the realistic simulations are more capable of representing the cloud field on large spatial scales, and appear to limit the aerosol perturbations leading to impacts on the thermodynamic conditions. Aerosol perturbations lead to changes in the cloud vertical structure, and thermodynamic evolution of the idealised simulations; a central feature of behavior seen previously in idealised simulations. Modelling approaches with open boundaries and time-varying forcing may allow for improved representation of shallow clouds in the atmosphere, and greater understanding of how they may respond to perturbations.

Plain Language Summary Clouds, and shallow clouds in particular, are responsible for much uncertainty in our understanding of the atmosphere, and the response of the climate system to anthropogenic perturbations. The representation of shallow clouds in models has long been a challenge due to the myriad processes and scales involved; from micrometer cloud droplets, to cloud fields of tens or hundreds of km, leading to many computational difficulties. Here we present and compare a number of simulations using different approaches. We show that certain modelling choices allow for an improved representation of shallow cloud fields on large scales, and also show a different response to aerosol perturbations, with implications for future development of estimations of the effects of aerosol on shallow clouds.

1. Introduction

Shallow cumuli play a number of important roles in trade wind regions, affecting both their local environment, and the climate as a whole. Low cloud feedbacks are responsible for much of the uncertainty in estimates of climate sensitivity (Bony & Dufresne, 2005; Bony et al., 2004; Boucher et al., 2013; Medeiros et al., 2008, 2015; Vial et al., 2013). One intensely studied aspect of shallow cumuli is how they are affected by changes in atmospheric aerosol, which facilitate the formation of cloud droplets by acting as cloud condensation nuclei (CCN) (Köhler, 1936). While certain aerosol effects on clouds are well understood, many questions, on scales varying from microphysical to entire cloud fields, remain open.

Higher concentrations of CCN lead to a greater number of smaller droplets, for a given liquid water content (Twomey, 1977). The greater droplet surface area increases scattered shortwave radiation, and thus cloud albedo. Smaller droplets due to increased aerosol may inhibit precipitation (Albrecht, 1989), and lead to longer cloud lifetimes. However, mechanisms have also been proposed for aerosol causing shorter lifetimes due to evaporation and entrainment feedbacks (Small et al., 2009).

Stevens and Feingold (2009) discuss “buffering” effects in the response of clouds to aerosol perturbations, where systems respond to offset the effect of the perturbation. For example, increased aerosol may suppress precipitation, allowing more moisture to be lifted to the cloud top, enhancing evaporative cooling and destabilising the cloud layer, causing clouds to deepen and produce more precipitation. Convective invigoration and deepening due to aerosol are supported by both observations and modelling (Albrecht, 1993; Dagan et al., 2016; Kaufman et al., 2005; Koren et al., 2014; Sheffield et al., 2015; Yuan et al., 2011), however some find suppression of convection (Jiang & Feingold, 2005; Xue et al., 2008). Van den Heever et al. (2011)

© 2021. The Authors.

This is an open access article under the terms of the [Creative Commons Attribution](https://creativecommons.org/licenses/by/4.0/) License, which permits use, distribution and reproduction in any medium, provided the original work is properly cited.

find that deeper cumulus modes, such as congestus, may be invigorated while the shallowest clouds are suppressed. Dagan et al. (2017) and Altaratz et al. (2014) suggest invigoration or suppression may depend on the magnitude of the aerosol perturbation, as well as local conditions. Seifert et al. (2015) discuss the deepening response of trade wind cumuli to aerosol perturbations as a transient effect, altering the thermodynamic environment, and eventually leading to a similar quasi-equilibrium cloud field. This quasi-equilibrium is considered as a regime of subsiding radiative-convective equilibrium (RCE), where prescribed large-scale forcings alter the state compared to traditional RCE. However, Dagan et al. (2018) find that typical cloud field lifetimes are much less than the time required to reach equilibrium, suggesting that such quasi-equilibrium behavior is unrealistic.

Much modelling work on shallow cumuli has used large eddy simulations (LES), typically with small domains on the order of tens of km, periodic lateral boundaries, and constant prescribed tendencies of winds, moisture, and thermodynamics. An alternative approach may be employed, whereby a global driving model supplies the forcing for a nested high resolution domain (Klocke et al., 2017; Miltenberger et al., 2018; Spill et al., 2019). Spill et al. (2019) find a similar form of cloud response to aerosol perturbations, however the convective deepening does not impact the thermodynamic state of the domain significantly, and no equilibrium cloud field is produced, in contrast to findings such as those of Seifert et al. (2015).

Here we build on Spill et al. (2019) by directly comparing this approach with one that is more idealised, similar to LES, using different configurations of the Met Office Unified Model (UM) to account for model uncertainty. We investigate the approaches' representation of the cloud field, and their response to aerosol perturbations, on large scales.

2. Methods

Our simulations are based on the Rain in Cumulus over the Ocean (Raubert et al., 2007) (RICO) campaign. RICO has long been a popular choice for studying shallow convection due to the prevalence of trade wind cumuli in the region, and the availability of data for model initialization and evaluation. Our case is initialised for 00:00UTC January 19, 2005, following Abel and Shipway (2007), with domains centred on 17.5°N, 57°W. All simulations are run for 96 h, including a 12 h spin-up.

Several configurations of the Met Office Unified Model are applied, with large domains of $\sim 500 \text{ km} \times \sim 500 \text{ km}$, a horizontal resolution of $\sim 500 \text{ m} \times \sim 500 \text{ m}$, and a stretched vertical coordinate system with 70 levels below 40 km, and 30 levels below 3 km. The UM uses a 3D Smagorinsky-type turbulence scheme (Boutle et al., 2014), and no convection scheme is enabled. The “realistic” setup uses a nested domain with open lateral boundaries, with boundary conditions supplied hourly by an external global driving configuration of the UM (vn11.1, GA6.1), run from ERA Interim (Dee et al., 2011) initial conditions. The “idealised” setup has periodic lateral boundaries, and constant large-scale tendencies of temperature and moisture are applied, as in most LES studies. Domain mean profiles of temperature, moisture, and winds from the realistic simulations are used to initialise the idealised simulations. Constant surface sensible and latent heat fluxes of 10.58 W m^{-2} and 93.17 W m^{-2} are prescribed, based on mean values of the time-varying fluxes in the realistic simulations. Horizontal advection of moisture, and large-scale subsidence are applied below 10 km following Abel and Shipway (2007), along with a cooling rate, a significant component of which is to account for radiative cooling (van Zanten et al., 2011). Idealised simulations are therefore performed both with and without a radiation scheme, to provide an extra point of comparison between idealised and realistic configurations. However, the scheme does not have a diurnal cycle, differing from the realistic simulations. Following Seifert et al. (2015), an advective cooling rate is applied in simulations including a radiation scheme. Profiles of idealised initial conditions and applied tendencies are shown in Figure 1.

Small domain idealised simulations are also performed, to more closely relate this comparison to existing LES studies. These have a domain of $\sim 50 \text{ km} \times \sim 50 \text{ km}$, a horizontal resolution of $\sim 100 \text{ m} \times \sim 100 \text{ m}$, and include the radiation scheme.

We use the double-moment microphysics scheme CASIM (Grosvenor et al., 2017; Miltenberger et al., 2018; Shipway & Hill, 2012), with a droplet activation scheme from Shipway (2015). The configuration of CASIM has a one-way coupling between cloud and aerosol, in which aerosol fields affect droplet activation and may

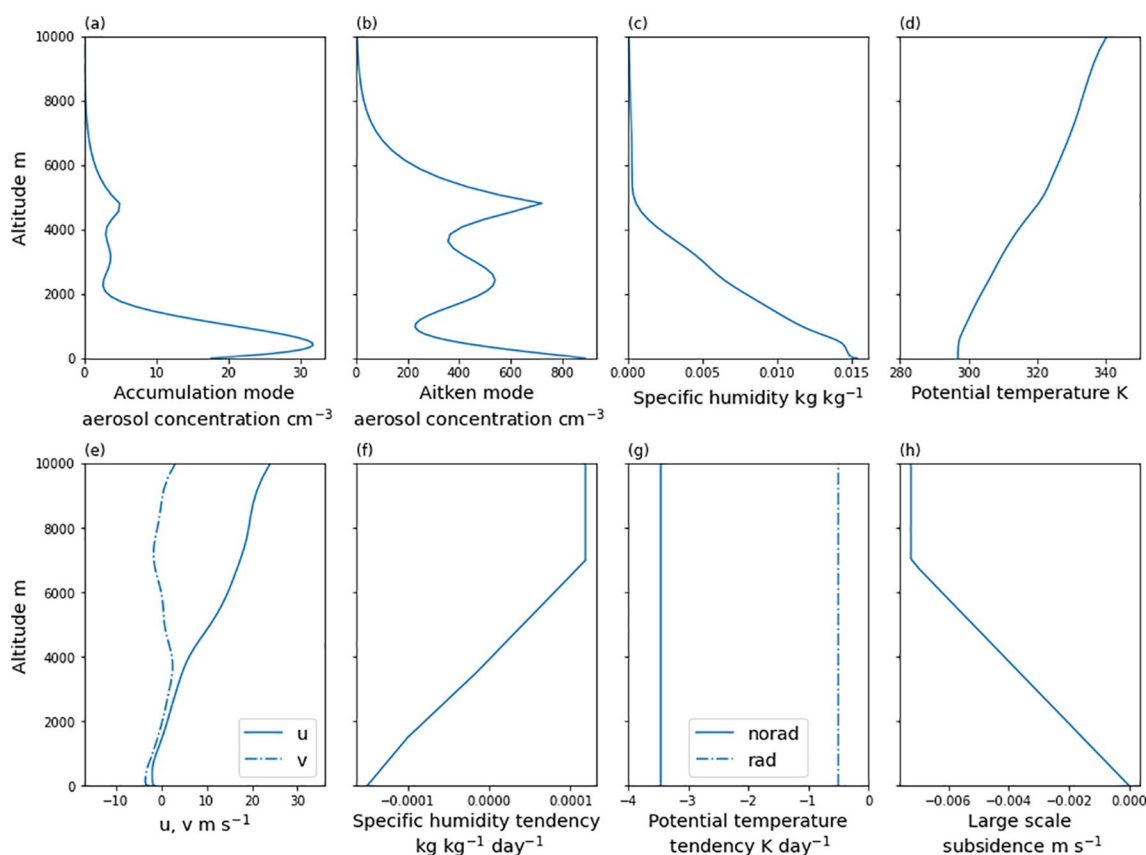


Figure 1. Profiles of prescribed aerosol and idealised initial conditions and tendencies (a),(b) baseline accumulation and Aitken mode aerosol concentrations (c, d, e) initial specific humidity, temperature, and winds (f), (g) tendencies of specific humidity and temperature (for idealised simulations with and without radiation schemes), (h) applied large-scale subsidence.

be advected, but are not affected by cloud microphysical processes. Aerosol profiles based on measurements during RICO, as described in Spill et al. (2019) and shown in Figure 1, are used for initial and lateral boundary conditions. Simulations are run with baseline aerosol profiles, and profiles perturbed by a factor of 10. The simulation names, along with key aspects of their configurations, are summarised in Table 1.

Table 1
Summary of Simulation Names and Configurations

Simulation	Domain size		Horizontal resolution		Lateral boundaries		Radiation scheme	Aerosol	
	$\sim 500\text{m} \times \sim 500\text{ km}$	$\sim 50\text{m} \times \sim 50\text{ km}$	$\sim 500\text{m} \times \sim 500\text{m}$	$\sim 100\text{m} \times \sim 100\text{m}$	Open	Periodic		Baseline	Perturbed ($\times 10$)
nested	Y		Y		Y		Y	Y	
nested_x10	Y		Y		Y		Y		Y
id_500 km_norad	Y		Y			Y		Y	
id_500 km_norad_x10	Y		Y			Y			Y
id_500 km_rad	Y		Y			Y	Y	Y	
id_500 km_rad_x10	Y		Y			Y	Y		Y
id_50 km_rad		Y		Y		Y	Y	Y	
id_50 km_rad_x10		Y		Y		Y	Y		Y

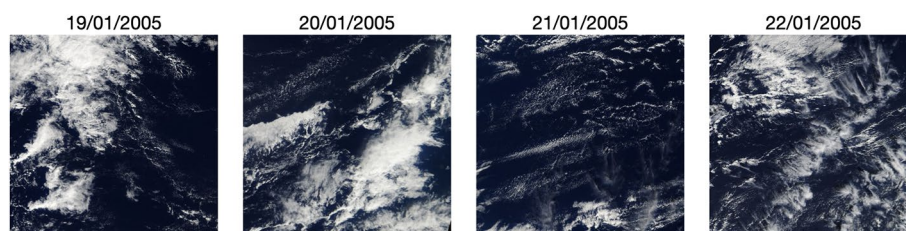


Figure 2. Satellite snapshots (Terra, MODIS, Corrected Reflectance, True Color, Bands 1-4-3) for the simulation days, showing the same domain as the nested simulations, from NASA Worldview Snapshots (<https://worldview.earthdata.nasa.gov/>).

3. Results

Satellite snapshots from the days of the simulations (Figure 2) show a great deal of structure and variability in the cloud field on large scales, including large features, even in this region that typifies trade wind cumuli. Comparing these with snapshots of the cloud fields from the realistic and idealised simulations in Figure 3, the large domain idealised simulations (Figures 3c–3f) produce a much more uniform cloud field than the realistic case (Figures 3a and 3b) and the satellite snapshots. While a relatively uniform cloud field may be expected over scales of tens of km, such uniformity over hundreds of km as seen in the large idealised domain is unlikely to be representative of the real atmosphere. The small domain simulations (Figures 3g and 3h) exhibit uniformity in some scenes, and more varied cloud fields in others. However, their smaller size makes this a more limited representation of the varied cloud fields. The idealised cloud fields appear to develop more structure later in the simulations, also shown by Seifert et al. (2015), though still to a lesser extent than the realistic simulations.

The simulations differ in their domain mean properties, and in these properties' response to the aerosol perturbations (Figure 4). Liquid water path increases with aerosol in all of the large domain simulations, particularly id_500 km_norad_x10, while id_50 km_rad_x10 shows an increase beginning in the second day. Precipitation is reduced with increased aerosol in the large domain idealised simulations, and through much of the first half of id_50 km_rad_x10. This effect is smaller in the realistic simulations.

Notably, the cloud fraction in the realistic simulations is completely agnostic to the aerosol perturbation, while each idealised setup shows an increase in cloud fraction with increased aerosol (Figure 4c).

Vertical profiles of cloud fraction, domain mean and in-cloud liquid water, and updraught speeds show clearly the simulations' differing structure and response to aerosol (Figure 5). The in-cloud profiles are, at their highest and lowest altitudes, dominated by relatively few instances in the simulations, but nonetheless provide insight into the in-cloud response. In the realistic simulations, these are a result of a number of large-scale, deeper, features. Applying a rolling filter, with a cloud-fraction threshold of 0.2, allows us to consider only a subset of smaller clouds, comparable to the idealised cloud fields. An alternative filter is applied to exclude clouds in the realistic simulations whose top heights exceed the maximum in the idealised simulations.

The idealised setups have larger mean in-cloud liquid water content (LWC) and updraught speeds, and display significant convective deepening and invigoration in response to increased aerosol, apparent in both domain mean and in-cloud profiles of LWC. While this effect is present in the realistic setup, it is muted in comparison. Applying the cloud-fraction threshold to the realistic simulations produces in-cloud profiles with a form similar to those in the idealised simulations, with more significant deepening than the unfiltered profile, though still less than the idealised simulations in the domain-mean. The cloud top height filter does little to affect the form of the profile, though produces slightly larger updraught speeds than the unfiltered profile.

Histograms of cloud top height (Figures 5e–5h) further highlight the differences in the cloud populations produced, and the response to increased aerosol. The occurrence of lower cloud top heights is suppressed in all perturbed simulations, though to a greater extent in nested_x10. All simulations also show an increase in the number of higher cloud top heights.

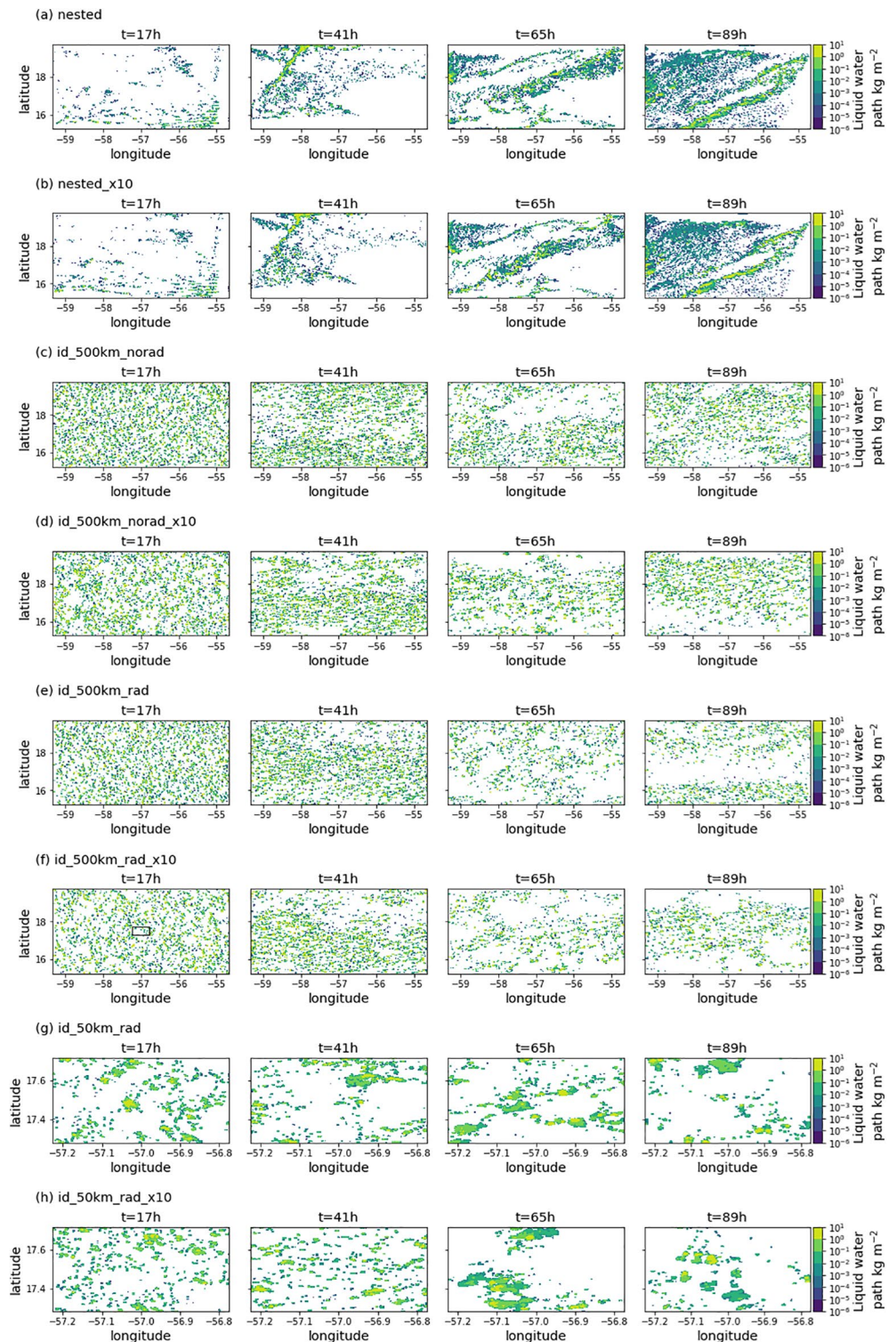


Figure 3. Snapshots of liquid water path at several times during each simulation (a), (b) nested simulations (c), (d) idealised simulations with no radiation scheme (e), (f) with radiation, and (g), (h) small domain idealised simulations. Note that (g), (h) use a different spatial scale due to the smaller domain size of $\sim 50 \text{ km} \times \sim 50 \text{ km}$, outlined in the first panel of (f).

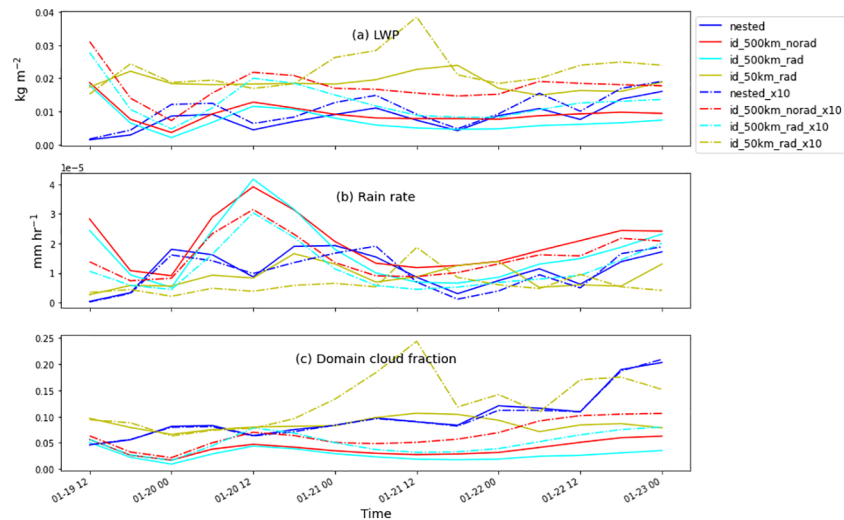


Figure 4. Timeseries of 6-hourly domain mean (a) liquid water path, (b) rain rate, (c) cloud fraction, for each simulation, starting after an initial 12 h spin-up.

Figure 6 shows the evolution of temperature and humidity profiles in each simulation. The stark contrast between the realistic and idealised setups, and their responses to the aerosol perturbation, is evident. The perturbed idealised simulations have increased cooling towards the top of and above the cloud layer, and increases in moisture at the top of the cloud layer. This is what one might expect to see from buffering effects; with greater cooling allowing the deepening of the cloud layer, and more moisture being lofted higher in the atmosphere (Albrecht, 1993; Dagan et al., 2016; Seifert et al., 2015). The realistic simulations, however, show almost no thermodynamic response to the aerosol perturbation, consistent with the muted deepening and invigoration response.

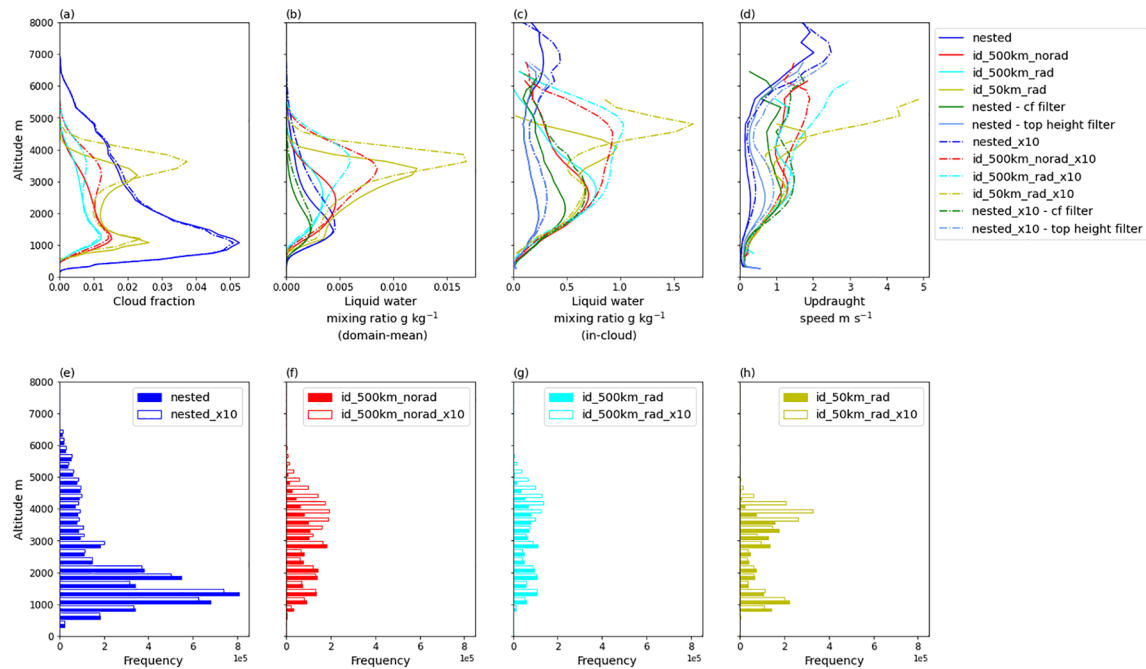


Figure 5. Vertical profiles of (a) cloud fraction, (b) domain mean cloud liquid water mixing ratio, (c) in-cloud mean liquid water mixing ratio, (d) updraught speed, and (e)–(h) histograms of cloud top height. A liquid water mixing ratio threshold of 0.01 g kg^{-1} is used to define a cloudy grid box. A rolling cloud fraction filter of 0.2, and a filter excluding clouds with top heights greater than maximum in the idealised simulations, are applied to the nested simulations, to produce additional profiles in (b)–(d), labelled with the suffixes “- cf. filter” and “- top height filter”.

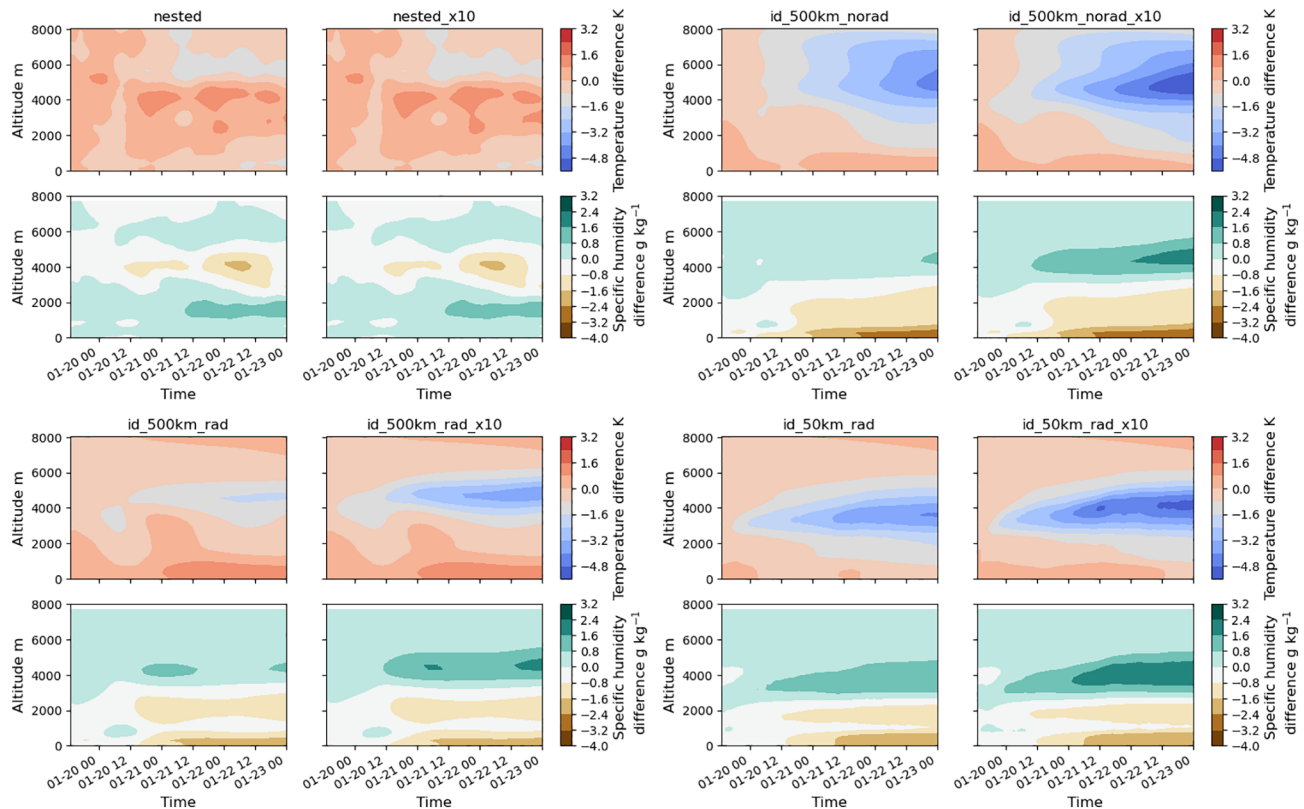


Figure 6. Hovmöller plots showing the temporal evolution of profiles of domain mean temperature and specific humidity. These show the difference between the mean temperature or specific humidity at each time in the simulation and the first time point after the 12 h spin-up. The nested and nested_x10 simulations are in the top left quadrant, id_500 km_norad and id_500 km_norad_x10 in the top right, id_500 km_rad and id_500 km_rad_x10 in the bottom left, and id_50 km_rad and id_50 km_rad_x10 in the bottom right.

4. Discussion

We have presented simulations of trade wind cumuli using different configurations of the Unified Model, highlighting the differences between idealised simulations, with fixed forcing and periodic boundaries, and more realistic simulations with open boundaries and varying large scale forcing. These configurations are chosen to eliminate as much model uncertainty as possible, and focus on examining the difference in aerosol-cloud interactions between the periodic domains with fixed forcing, and nested domains with varying forcing.

Snapshots of liquid water path show that the idealised and realistic simulations produce dramatically different cloud fields over large scales. The realistic simulations produce cloud fields with more evident structure, while the idealised simulations produce notably more uniform cloud fields. Domain mean liquid water path, precipitation, and cloud fraction further highlight the differences between the response to aerosol perturbations. The realistic simulations show no change in cloud fraction in response to increased aerosol, in contrast to the increase in the idealised simulations.

Vertical profiles of cloud liquid water indicate that the idealised simulations experience significantly more convective deepening with increased aerosol. While realistic and idealised may produce clouds with similar structures, the response to the aerosol perturbation of those in the realistic simulations is much weaker.

The thermodynamic evolution of the domain is driven by the applied large-scale forcing, and processes including interactions between the clouds and their environment, which are closely coupled to the cloud vertical structure. In the idealised simulations, increased aerosol leads to marked changes in the thermodynamic evolution, as would be expected from the buffering mechanism discussed by (Stevens & Feingold, 2009). No significant changes are seen in the thermodynamic evolution of the realistic simulations.

This suggests that the thermodynamic environment is determined predominately by the varying large-scale forcing, which, along with the open boundaries, does not allow the cloud field to exert such a strong effect. However, it should be noted that the large-scale forcing and boundary conditions supplied by the driving model are not affected by the aerosol perturbation. Aerosol effects are thus only realised inside the nested domain, while in the real atmosphere this may not be the case. Nonetheless, observational studies have reached similar conclusions regarding the significance of transient large-scale forcing in determining the state of the cloud field. Dagan et al. (2018) show that cloud field properties and environmental conditions vary significantly over periods shorter than those required to reach an idealised equilibrium state.

Limited area idealised models are undoubtedly useful in studying atmospheric processes. However, our findings suggest that their ability to represent the transient behavior of the real atmosphere may be limited in comparison to more realistic approaches.

Aerosol perturbations may have a number of effects on cumulus cloud fields, including minor convective deepening and invigoration, and increases in liquid water path. However, due to the importance of the large-scale forcing, these are limited, perhaps explaining the unchanged cloud fraction.

Understanding the role of shallow clouds in the atmosphere is of critical importance, and with ever improving capabilities and methods, so too is understanding the differences, shortcomings, and advantages of modelling approaches.

Data Availability Statement

The simulation data used in this study was produced using the Met Office Unified Model, vn11.1. ERA Interim reanalysis was used to initialise the model, produced by the European Centre for Medium-range Weather Forecast (ECMWF) (2011): The ERA-Interim reanalysis data set, Copernicus Climate Change Service (C3S) (accessed 24/03/2017), available from <https://www.ecmwf.int/en/forecasts/datasets/archive-datasets/reanalysis-datasets/era-interim>. Simulation data used for the presented results are available at <https://doi.org/10.5281/zenodo.4805474>. The MODIS data used are available at <https://worldview.earthdata.nasa.gov/>. The aerosol data used are as shown in Spill et al. (2019).

Acknowledgments

This work used Monsoon2, a collaborative High Performance Computing facility funded by the Met Office and the Natural Environment Research Council. George Spill acknowledges funding from the Natural Environment Research Council with grant reference number 1796357, and from the UK Met Office. Guy Dagan and Philip Stier acknowledge funding from the European Research Council project RECAP under the European Union's Horizon 2020 research and innovation program with grant agreement 724602. Philip Stier additionally acknowledges funding from the Natural Environment Research Council project NE/P013406/1 (A-CURE), and funding from the European Union's Horizon 2020 research and innovation programme under grant agreement No 821205 (FORCES).

References

- Abel, S. J., & Shipway, B. J. (2007). A comparison of cloud-resolving model simulations of trade wind cumulus with aircraft observations taken during *rico*. *Quarterly Journal of the Royal Meteorological Society*, 133(624), 781–794. <https://doi.org/10.1002/qj.55>
- Albrecht, B. A. (1989). Aerosols, cloud microphysics, and fractional cloudiness. *Science*, 245(4923), 1227–1230. <https://doi.org/10.1126/science.245.4923.1227>
- Albrecht, B. A. (1993). Effects of precipitation on the thermodynamic structure of the trade wind boundary layer. *Journal of Geophysical Research*, 98, 7327–7337. <https://doi.org/10.1029/93jd00027>
- Altartatz, O., Koren, I., Remer, L. A., & Hirsch, E. (2014). Review: Cloud invigoration by aerosols—Coupling between microphysics and dynamics. *Atmospheric Research*, 140, 38–60. <https://doi.org/10.1016/j.atmosres.2014.01.009>
- Bony, S., & Dufresne, J.-L. (2005). Marine boundary layer clouds at the heart of tropical cloud feedback uncertainties in climate models. *Geophysical Research Letters*, 32(20). <https://doi.org/10.1029/2005gl023851>
- Bony, S., Dufresne, J.-L., Le Treut, H., Morcrette, J.-J., & Senior, C. (2004). On dynamic and thermodynamic components of cloud changes. *Climate Dynamics*, 22(2), 71–86. <https://doi.org/10.1007/s00382-003-0369-6>
- Boucher, O., Randall, D., Artaxo, P., Bretherton, C., Feingold, G., Forster, P., & Zhang, X. Y. (2013). Clouds and Aerosols. *Climate change 2013: The physical science basis. Contribution of working group i to the fifth assessment report of the intergovernmental panel on climate change* (pp. 571–658). Cambridge University Press. <https://doi.org/10.1017/CBO9781107415324.016>
- Boutle, I. A., Eyre, J. E. J., & Lock, A. P. (2014). Seamless stratocumulus simulation across the turbulent gray zone. *Monthly Weather Review*, 142(4), 1655–1668. <https://doi.org/10.1175/mwr-d-13-00229.1>
- Dagan, G., Koren, I., Altartatz, O., & Heiblum, R. H. (2016). Aerosol effect on the evolution of the thermodynamic properties of warm convective cloud fields. *Scientific Reports*, 6, 38769. <https://doi.org/10.1038/srep38769>
- Dagan, G., Koren, I., Altartatz, O., & Heiblum, R. H. (2017). Time-dependent, non-monotonic response of warm convective cloud fields to changes in aerosol loading. *Atmospheric Chemistry and Physics*, 17(12), 7435–7444. <https://doi.org/10.5194/acp-17-7435-2017>
- Dagan, G., Koren, I., Altartatz, O., & Lehahn, Y. (2018). Shallow convective cloud field lifetime as a key factor for evaluating aerosol effects. *iScience*, 10, 192–202. <https://doi.org/10.1016/j.isci.2018.11.032>
- Dee, D. P., Uppala, S. M., Simmons, A. J., Berrisford, P., Poli, P., Kobayashi, S., et al. (2011). The era-interim reanalysis: configuration and performance of the data assimilation system. *Quarterly Journal of the Royal Meteorological Society*, 137(656), 553–597. <https://doi.org/10.1002/qj.828>
- Grosvenor, D. P., Field, P. R., Hill, A. A., & Shipway, B. J. (2017). The relative importance of macrophysical and cloud albedo changes for aerosol-induced radiative effects in closed-cell stratocumulus: Insight from the modelling of a case study. *Atmospheric Chemistry and Physics*, 17(8), 5155–5183. <https://doi.org/10.5194/acp-17-5155-2017>

- Jiang, H., & Feingold, G. (2005). Effect of aerosol on warm convective clouds: Aerosol-cloud-surface flux feedbacks in a new coupled large eddy model. *Journal of Geophysical Research*, 111(D1). <https://doi.org/10.1029/2005JD006138>
- Kaufman, Y. J., Koren, I., Remer, L. A., Rosenfeld, D., & Rudich, Y. (2005). The effect of smoke, dust, and pollution aerosol on shallow cloud development over the Atlantic Ocean. *Proceedings of the National Academy of Sciences*, 102(32), 11207–11212. <https://doi.org/10.1073/pnas.0505191102>
- Klocke, D., Brueck, M., Hohenegger, C., & Stevens, B. (2017). Rediscovery of the doldrums in storm-resolving simulations over the tropical atlantic. *Nature Geoscience*, 10(12), 891–896. <https://doi.org/10.1038/s41561-017-0005-4>
- Köhler, H. (1936). The nucleus in and the growth of hygroscopic droplets. *Transactions of the Faraday Society*(32), 1152–1161. <https://doi.org/10.1039/tf9363201152>
- Koren, I., Dagan, G., & Altartatz, O. (2014). From aerosol-limited to invigoration of warm convective clouds. *Science*, 344(6188), 1143–1146. <https://doi.org/10.1126/science.1252595>
- Medeiros, B., Stevens, B., & Bony, S. (2015). Using aquaplanets to understand the robust responses of comprehensive climate models to forcing. *Climate Dynamics*, 44(7), 1957–1977. <https://doi.org/10.1007/s00382-014-2138-0>
- Medeiros, B., Stevens, B., Held, I. M., Zhao, M., Williamson, D. L., Olson, J. G., & Bretherton, C. S. (2008). Aquaplanets, climate sensitivity, and low clouds. *Journal of Climate*, 21(19), 4974–4991. <https://doi.org/10.1175/2008JCLI1995.1>
- Miltenberger, A. K., Field, P. R., Hill, A. A., Rosenberg, P., Shipway, B. J., Wilkinson, J. M., et al. (2018). Aerosol–cloud interactions in mixed-phase convective clouds – Part 1: Aerosol perturbations. *Atmospheric Chemistry and Physics*, 18(5), 3119–3145. <https://doi.org/10.5194/acp-18-3119-2018>
- Rauber, R. M., Stevens, B., Ochs, H. T., Knight, C., Albrecht, B. A., Blyth, A. M., et al. (2007). Rain in shallow cumulus over the ocean: The rico campaign. *Bulletin of the American Meteorological Society*, 88(12), 1912–1928. <https://doi.org/10.1175/BAMS-88-12-1912>
- Seifert, A., Heus, T., Pincus, R., & Stevens, B. (2015). Large-eddy simulation of the transient and near-equilibrium behavior of precipitating shallow convection. *Journal of Advances in Modeling Earth Systems*, 7(4), 1918–1937. <https://doi.org/10.1002/2015ms000489>
- Sheffield, A. M., Saleeby, S. M., & Heever, S. C. (2015). Aerosol-induced mechanisms for cumulus congestus growth. *Journal of Geophysical Research: Atmosphere*, 120(17), 8941–8952. <https://doi.org/10.1002/2015jd023743>
- Shipway, B. J. (2015). Revisiting twomey's approximation for peak supersaturation. *Atmospheric Chemistry and Physics*, 15(7), 3803–3814. <https://doi.org/10.5194/acp-15-3803-2015>
- Shipway, B. J., & Hill, A. A. (2012). Diagnosis of systematic differences between multiple parametrizations of warm rain microphysics using a kinematic framework. *Quarterly Journal of the Royal Meteorological Society*, 138(669), 2196–2211. <https://doi.org/10.1002/qj.1913>
- Small, J. D., Chuang, P. Y., Feingold, G., & Jiang, H. (2009). Can aerosol decrease cloud lifetime? *Geophysical Research Letters*, 36(16). <https://doi.org/10.1029/2009gl038888>
- Spill, G., Stier, P., Field, P. R., & Dagan, G. (2019). Effects of aerosol in simulations of realistic shallow cumulus cloud fields in a large domain. *Atmospheric Chemistry and Physics*, 19(21), 13507–13517. <https://doi.org/10.5194/acp-19-13507-2019>
- Stevens, B., & Feingold, G. (2009). Untangling aerosol effects on clouds and precipitation in a buffered system. *Nature*, 461, 607–613. <https://doi.org/10.1038/nature08281>
- Twomey, S. (1977). The influence of pollution on the shortwave albedo of clouds. *Journal of the Atmospheric Sciences*, 34(7), 1149–1152. [https://doi.org/10.1175/1520-0469\(1977\)034<1149:TIOPOT>2.0.CO;2](https://doi.org/10.1175/1520-0469(1977)034<1149:TIOPOT>2.0.CO;2)
- van den Heever, S. C., Stephens, G. L., & Wood, N. B. (2011). Aerosol indirect effects on tropical convection characteristics under conditions of radiative–convective equilibrium. *Journal of the Atmospheric Sciences*, 68(4), 699–718. <https://doi.org/10.1175/2010JAS3603.1>
- van Zanten, M. C., Stevens, B., Nuijens, L., Siebesma, A. P., Ackerman, A. S., Burnet, F., et al. (2011). Controls on precipitation and cloudiness in simulations of trade-wind cumulus as observed during rico. *Journal of Advances in Modeling Earth Systems*, 3(2). <https://doi.org/10.1029/2011MS000056>
- Vial, J., Bony, S., Dufresne, J.-L., & Roehrig, R. (2013). Coupling between lower-tropospheric convective mixing and low-level clouds: Physical mechanisms and dependence on convection scheme. *Journal of Advances in Modeling Earth Systems*, 5(4), 1892–1911. <https://doi.org/10.1002/2016MS000740>
- Xue, H., Feingold, G., & Stevens, B. (2008). Aerosol effects on clouds, precipitation, and the organization of shallow cumulus convection. *Journal of the Atmospheric Sciences*, 65(2), 392–406. <https://doi.org/10.1175/2007JAS2428.1>
- Yuan, T., Remer, L. A., & Yu, H. (2011). Microphysical, macrophysical and radiative signatures of volcanic aerosols in trade wind cumulus observed by the a-train. *Atmospheric Chemistry and Physics*, 11(14), 7119–7132. <https://doi.org/10.5194/acp-11-7119-2011>